Biointerface Research in Applied Chemistry
Open-Access Journal (ISSN: 2069-5837)

Article
Volume 13, Issue 4, 2023, 373
https://doi.org/10.33263/BRIAC134.373

Hydroxyapatite Modified Silica Aerogel Nanoparticles: *In Vitro* Cell Migration Analysis

Nor Suriani Sani [1], Nik Ahmad Nizam Nik Malek [2,3,*]

[1] Office of Deputy Vice-Chancellor (Research and Innovation), Universiti Teknologi Malaysia, 81310 UTM, Skudai, Johor, Malaysia; norsuriani@utm.my (N.S.S);
[2] Centre for Sustainable Nanomaterials (CSNano), Ibnu Sina Institute for Scientific and Industrial Research (ISI-ISIR), Universiti Teknologi Malaysia, 81310 UTM Johor, Malaysia; niknizam@utm.my (N.A.N.N.M);
[3] Department of Biosciences, Faculty of Science, Universiti Teknologi Malaysia, 81310 UTM, Skudai, Johor, Malaysia
* Correspondence: niknizam@utm.my;

Scopus Author ID 35995651900
Received: 16.02.2022; Accepted: 21.03.2022; Published: 7.10.2022

Abstract: The ability of silica aerogel nanoparticles (SA-Np) to improve the stability of hydroxyapatite (HA) was investigated. Using the sol-gel method, the HA was incorporated into SA-Np at a weight ratio of 0.5 of HA to SiO_2 (HA-SA-Np). The efficacy of HA-SA-Np, SA-Np, and HA on the *in vitro* migration of normal human dermal fibroblast cells (HSF1184) was compared. The cell migration was measured at 0, 6, and 24 hours after scratching using ImageJ and an inverted optical microscope. To ascertain the resorbability of HA-SA-Np, the phosphate and silicic acid concentrations in media treated for 2, 5, and 7 days were examined. The high dissolution of HA could be reduced by incorporating the HA into the silica nanosphere. The HA-SA-Np significantly stimulated cell migration and increased closure with increasing treatment time. It was caused by the release of silicic acid, which aided in healing cells. It also demonstrates the ability of HA-SA-Np to be resorbed and eventually increase the adhesion and migration of normal human fibroblast cells. As a result, the potential application of HA-SA-Np as an alternative biomaterial was confirmed.

Keywords: hydroxyapatite; silica aerogel; incorporation; cell migration; biomaterial.

1. Introduction

Following an injury, several biological processes are involved in restoring the normal integrity of the skin. Wound healing is critical for restoring the skin's barrier function. During this procedure, cells at the wound's edges multiply and move around, re-epithelializing the wound surface [1]. The capacity of cells to move allows them to alter their position within tissues or between organs [2]. Parts of the skin must be replaced after severe burns. However, the number of skin donors available may be insufficient for routine wound healing. Bioactive therapeutic delivery, cell therapy, and biomaterial application for skin tissue engineering are just a few of the many strategies and approaches for improving wound healing [2-4]. On that note, appropriate biomaterials can be used to regenerate skin cells [4].

According to Ocando *et al*. [5], the green chemistry approach to biomaterials can be performed using hydroxyapatite (HA), which has a similar composition to bone. HA is mainly employed as a bone implant and in periodontal therapy because of its superior bioactivity and osteoconductivity [6]. However, when compared to other bioactive materials, HA has some disadvantages. Despite its high biocompatibility and bioactivity, HA is naturally brittle and

resorbable [3,7]. To maintain results, HA-based fillers must be reinjected annually. However, this typically results in edema at the injection site [8], limiting the material's clinical applicability.

The positive effect of silica on cell growth [9] intrigued researchers' interest in working on silica-substituted HA as an advanced bioactive ceramic [10]. Silica has been linked to improved HA biocompatibility [11]. This released phenomenon positively influences cells due to silanol groups and silica resorption during treatment [3,9]. The rate of cell apposition into the bioceramic has greatly increased due to silica's incorporation into HA [12,13]. Silica-based biomaterials promote angiogenesis by releasing silicate ions, which increase the expression of proangiogenic factors [14]. The 3-dimensional silica nonwoven fabrics have promoted cultured cell growth and tissue formation [15,16]. As a result, a strategy for improving wound healing in humans can be implemented by using a hydroxyapatite-silica composite, as both materials have specific functions as biomaterials.

Previous research has shown that the HA-incorporated silica aerogels nanoparticles (HA-SA-Np) can be synthesized using a sol-gel technique from rice hull ash as the silica precursor via ambient pressure drying [3,17,18]. During the sol-gel method, HA was added to the silica gel at appropriate synthesis parameters [3,17,18]. Silica aerogel nanoparticles (SA-Np) are not cytotoxic to human cells and can increase normal human fibroblast *in vitro* when compared to untreated cells (raw cells) *in vitro* [17]. According to previous findings, the HA and SA-Np ratios in the HA-SA-Np influenced cell viability (normal human fibroblast and osteoblast cells). The silica-deficient composite (HA/SiO_2 ratio >1.0) did not affect cell viability, whereas the silica-rich composite (HA/SiO_2 ratio 0.05-0.5) did [3,17]. The HA-SA-Np with the highest cell viability had a HA/SiO_2 ratio of 0.5, which has the best properties of both HA and silica.

Human dermal fibroblasts are the most common type of skin cell in the dermal layer. Furthermore, dermal fibroblasts are essential in cell regeneration and wound healing. A promising biomaterial, HA-SA-Np, was developed to have better mechanical, biocompatibility, and bio-functionality characteristics [3,17]. As a carrier and cell delivery vehicle for implants and wound care applications, it was expected that HA-SA-Np production at the ideal ratio of incorporated HA and SA-Np would be used [11,19]. The effectiveness and capabilities of HA-SA-Np against typical human dermal fibroblast cells (HSF 1184) were investigated to confirm these hypotheses. It is critical to investigate further HA-SA-Np's ability to promote cell proliferation and migration and its function as a biomaterial for wound healing. The current study used cell migration assays to examine the effect of treated samples on the migration and healing ability of normal human fibroblast cells on different days. The cell migration assay was used because the migration phase is a control event during wound healing.

2. Materials and Methods

2.1. In vitro cell migration study.

According to earlier descriptions [3,17,18], silica aerogel nanoparticles (SA-Np) and hydroxyapatite (HA) incorporated silica aerogel nanoparticles with a HA/SiO_2 ratio of 0.5 (HA-SA-Np) were synthesized. The SA-Np and HA-SA-Np were synthesized from rice husk ash (a silica source) using an aqueous sol-gel ambient pressure drying process. The previous articles [3,17,18] also contain information on each instrumentation technique. The prepared

samples (SA-Np, HA-SA-Np, and HA) were tested for cell migration *in vitro* against normal human fibroblast cells.

The impact of the sample on the migration and healing capacity of HSF 1184 was examined using a cell migration test. This test began with rinsing the HA-SA-Np disc (0.1 mm height, 13 mm diameter) with 1 phosphate buffer solution (PBS) before sterilizing it under a UV lamp for 30 minutes on each side. After being sterilized, the disc was placed in 1 mL of complete Dulbecco's modified Eagle's medium (DMEM) and incubated for 2, 5, and 7 days. Following the procedure, the media were filtered and kept at 4°C. In 6-well microtiter plates with 2.0 mL each well and 1.0×10^6 fibroblast cells per well, the cells were planted and cultured at 37°C in a 5% CO_2 environment. After 24 hours of incubation, a tiny point was used to make an artificial wound gap by scratching the confluent monolayer of cells. The previously treated medium was added to the cells along with the samples. To obtain the same area during image acquisition, the outer bottom of each well was marked with an ultrafine tip marker. The marked site was used as a reference point close to the scratch area. The movement of scratched cells near the edge towards the gap's closure determined the ability of samples to stimulate healing. Within 24 hours, the image was captured at regular intervals [20]. Photos of the plates were obtained using an inverted optical microscope (Nikon Eclipse TS100) at the precise spot after 0, 6, 12, 18, and 24 hours. Three images were analyzed for each scratched area, and five points were taken for each sample. Both SA-Np and HA were used in the experiment, and the results were compared.

ImageJ 1.50i was used to quantify the healing and migration behavior of HSF 1184 cells (National Institute of Health, Bethesda, MD, USA). The total distance from the edge of the artificial wound toward the centre of the scratch until new cell-cell contacts were used to calculate the closure area. An untreated cell was used as a control. The following formula [20] was used to calculate the closure area:

$$Closure\ Area\ (\%) = \frac{Scratch\ Area_0 - Scratch\ Area_i}{Scratch\ Area_0}\ x\ 100;\ i = 6, 12, 24\ hours \quad (1)$$

2.2. Phosphate and silicic acid analyses.

The amounts of phosphate and silicic acid in the media after 2, 5, and 7 days of treatment were used to assess HA-SA-Np's resorbability. After incubation, the residual media were analyzed for phosphate and silicic acid. Because these ions are essential components of the HA and SA-Np frameworks, their presence in the media could suggest that the framework is dissolving. The concentrations (mg/L) of phosphate ion and silicic acid in the media after several days of culturing (the liquid component) were determined using Macherey-Nagel NANOCOLOR® UV-Vis spectrophotometer and Method 1-77 for phosphate, and Method 1-48 for silicic acid (silica) assay kits. The silicic acid content of the solution was determined using a reagent kit set with reference number 91848 (silica). A precise 20 mL sample was pipetted into a volumetric flask with a capacity of 25 mL. After that, 1 mL of R1 (acid sulphuric, H_2SO_4, 5-15%) was added, stirred, and set aside for 3 minutes. Then, reagent R2 (10-25 % sodium disulfide, $Na_2O_5S_2$) was added and adequately mixed. 1 mL of reagent R3 was added after 1 minute. The blank was made by substituting deionized water for the sample,

and the reagents were added similarly. The blank and test samples' volumetric flasks were then filled to the 25 mL mark with deionized water. After 15 minutes in a 10 mm cuvette at the 690 nm wavelength, measurements were taken with a NANOCOLOR® Vis spectrophotometer.

The process for determining phosphate followed Method 1-77, nanocolor. A reagent kit set with the reference number 91877 was used for this procedure. A 25 mL volumetric flask was filled with a pipette of 20 mL of the test sample, and the blank was distilled water. Following that, 1 mL of R1 reagent (acid sulphuric, H_2SO_4, 30%) from the kit was added and thoroughly mixed with the sample and blank. 1 mL R2 reagent (sodium disulfide, $Na_2O_5S_2$, 25%) was added one at a time, with thorough mixing. The volumetric flasks of the blank and test samples were then filled to the 25 mL mark with deionized water. To ensure a perfect mixing, the flask was lightly swirled. After 10 minutes, the mixture was poured into a 10 mm cuvette and analyzed at a wavelength of 690 nm with a NANOCOLOR® Vis spectrophotometer (Macherey-Nagel, Germany). The following formula [9] was used to determine the percentage loss of each element using UV-Vis spectrophotometric data:

$$\%\ Element_{loss} = \frac{Mean\ [E]_{mgL^{-1}}\ untreated\ solution - Mean\ [E]_{mgL^{-1}}\ treated\ solution}{Mean\ [E]_{mgL^{-1}}\ untreated\ solution} x100 \quad (2)$$

3. Results and Discussion

3.1. Cell migration of SA, HA-SA-Np, and HA.

The migrating behavior of the cells will provide insight into the bio-functionality of SA-Np and HA-SA-Np as skin-replacement materials, as well as an indicator for cell adherence, with higher adhesion leading to better proliferation. Figure 1 depicts the migration and adhesion of scratched HSF1184 cells that were exposed to medium with (a) untreated and (b) SA, (c) HA-SA-Np, and (d) HA that were treated at 7 days.

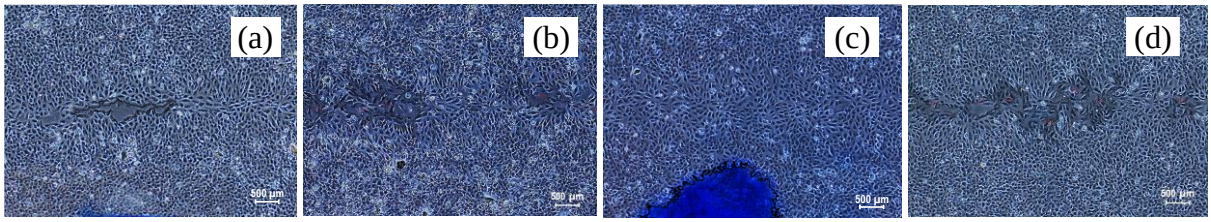

Figure 1. Pictures of the HSF 1184 cells migrating after being scratched for 24 hours. The scratched HSF1184 cells were subjected to the medium: **(a)** untreated, **(b)** SA, **(c)** HA-SA-Np, and **(d)** HA that was treated at 7 days. The exact location of the scratch spot was marked using the mark at the bottom of these images. The photos were captured using an inverted optical microscope, a scale bar of 500 m, and a magnification of 4/0.13.

After being treated with HA-SA-Np, SA, and free HA samples, the cells moved and formed cell-to-cell contact, as shown in Figure 1. After 24 hours of scratching, fibroblastic migration of SA, HA-SA-Np, and HA-treated samples was comparable to the control. The micrograph revealed that all of the substances were capable of considerably promoting cell motility. After 24 days of scratching, the migration gap treated with SA and HA was approximately the same size, but the cell thickness and density differed. HA-treated cells spread less and only partially covered the regions than SA-treated cells. The cells may require a longer cultivating time to fill the gap and attain a confluent monolayer stage. Figure 1(c) showed that the cells treated with HA-SA-Np were evenly distributed and that the scratched

gap was successfully closed after 24 hours of scratching. After 24 hours of scratching, the micrograph revealed that the cells were healthy, unharmed, continued to proliferate, became confluent, and eventually formed a monolayer coverage.

These findings show that the HA-SA-Np can boost normal human dermal fibroblast cell proliferation and tissue creation. The current results further suggest that successfully incorporating HA into the SA networks aided cell proliferation and migration. To test the sample's resorbable qualities on HSF 1184 cells, the study analyzed the phosphate ion and silicic acid concentrations (mg/L) in the media. Figure 2 shows the phosphate and silicic acid concentrations in the medium after 7 days of SA, HA-SA-Np, and HA treatment.

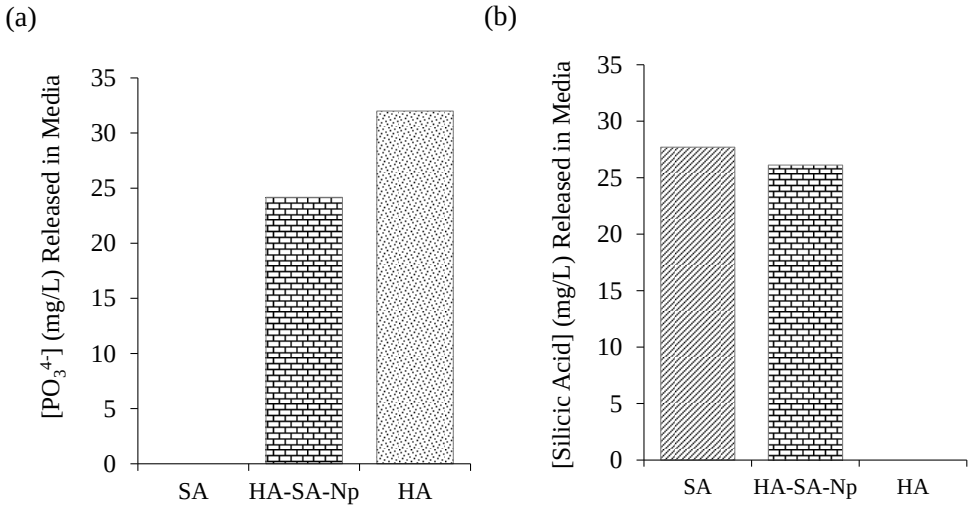

Figure 2. Concentration (mg/L) of **(a)** silicic acid and **(b)** phosphate ion released into media after 7 days treated with SA, HA-SA-Np, and HA.

The phosphate concentrations in the medium after 7 days of treatment are shown in Figure 2(a). The highest phosphate content was found in HA, indicating a fast release of phosphate ions into the medium. In an environment with increased phosphate concentrations, there is mutual competition amongst cells to interact with phosphate ions. Nonetheless, the cells' availability is limited in the early stages of incubation. As a result, the cells consumed a large number of phosphate ions, affecting cell development and slightly inhibiting the proliferation of cells treated with HA, as demonstrated by the cell migration test (Figure 1(d)) [21]. Figure 2 also revealed that cells treated with HA-SA-Np consumed an optimal quantity of phosphate ions in the media, migrated quicker, and closed the gap faster than cells treated with SA and HA, as indicated in Figure 1(c). This graph also shows that covering HA particles with the SA network delayed the high phosphate release from free HA [17].

Figure 2(b) depicts the release of silicic acid into the media during 7 days of incubation. Silicic acid was released from the SA and HA-SA-Np samples; however, it was not found in the HA sample. Cell migration on the HA-SA-Np and SA was more significant than HA during early cell growth (Figure 1), indicating that silica plays a vital role in promoting cell growth at the molecular level [9]. Figure 2(b) further reveals that the concentration of silicic acid released from SA was somewhat higher than HA-SA-Np after 7 days of treatment. After 24 hours of scratching, the cell migration was reduced after being treated with SA compared to HA-SA-Np, as shown in Figure 1. As a result of the extended incubation period (7 days), SA released a more significant concentration of silicic acid into the media than HA-SA-Np, which considerably slowed cell development.

The current findings back up previous research, which found that silica concentration in the media altered proliferative response [3,9-11]. These findings concluded that an adequate amount of silica plays a critical function in promoting cell growth at the molecular level during the early stages of proliferation. Despite the necessity for long culturing days, maintaining vital cellular processes required an optimal amount of phosphate ion [22]. It also shows that covering HA with SA networks delayed the high release of phosphate from HA and the high release of silicic acid from SA, which improved the biocompatibility and bio-functionality of this HA-SA-Np. These particular needs can be primarily met by producing HA-SA-Np, as demonstrated in this study.

3.2. Cell migration of HA-SA-Np.

The impact of HA-SA-Np (1 g/mL) on the migration of HSF 1184 cells was further investigated using a cells migration assay by exposing the cells to HA-SA-Np on various days (2, 5, and 7 days). HSF 1184 cells migrated microscopically at 0, 6, and 12 hours (Figure 3), and ImageJ was used to determine their closure rate (Figure 4).

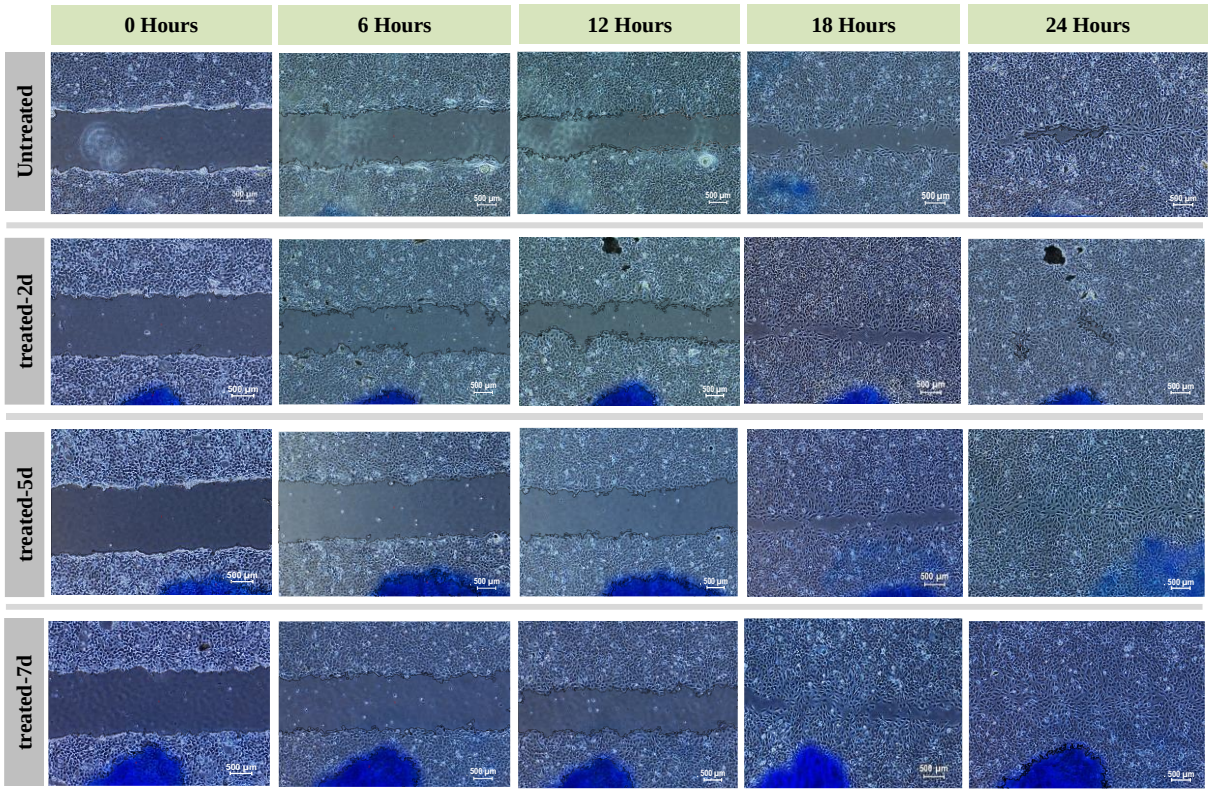

Figure 3. Photos of the HSF 1184 cells migrating at 0, 6, 12, 18, and 24 hours after scratching. The scratched HSF1184 cells were left untreated and subjected to the medium that had been HA-SA-Np-treated at different times (2, 5, and 7 days). The identical area of the scratch site was marked using the mark at the bottom of these images. The photos were captured using an inverted optical microscope with a scale bar of 500 m and a magnification of 4/0.13.

The fibroblast cells treated with HA-SA-Np had considerably increased cell proliferation and migration compared to the untreated sample. HA-SA-Np significantly (p 0.001-p 0.0001) increased cell migration after 24 hours of scratching (Figure 4). The closure area was influenced by the various treatment times, and a direct link with treated time was observed, as shown in Figure 3.

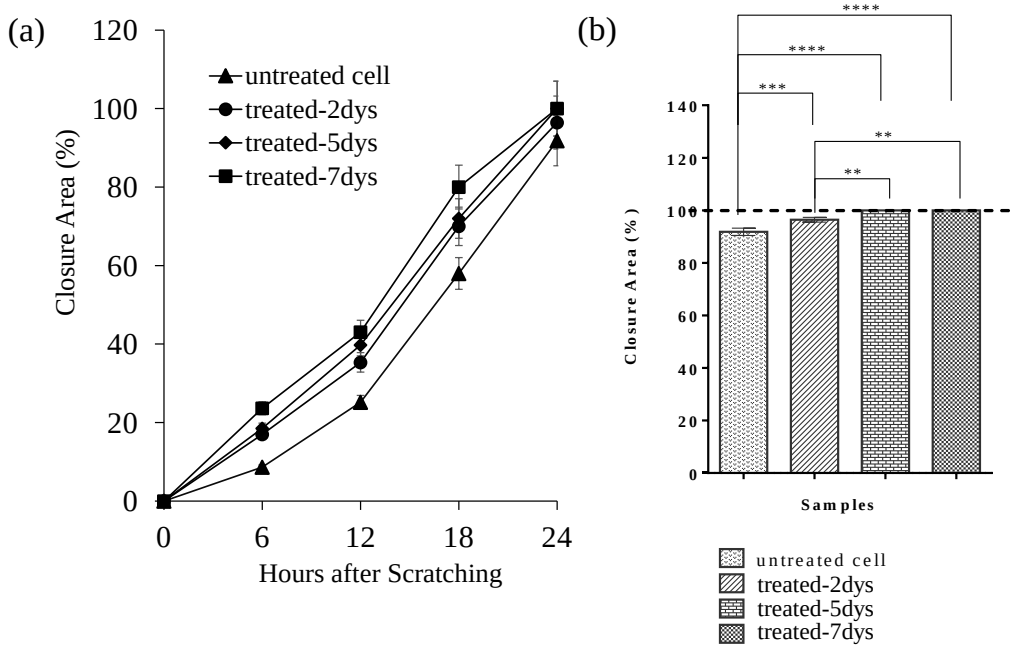

Figure 4. (a) The percentage of HSF 1184 cells with closed areas after 0, 6, 12, and 24 hours of scratching. **(b)** The percentage of HSF 1184 cells with closed areas following 24 hours of scratching. Data are shown as the mean and standard deviation (SD) of three separate studies. Using one-way ANOVA, the following comparisons with other samples have **P 0.01, ***P 0.001, and ****P 0.0001.

The treatment with treated-2ys (media treated with HA-SA-Np for 2 days) resulted in the closure of an estimated 17 percent of the scratched region 6 hours after scratching. The closure area grew to 24 percent when the treatment duration was increased from 5 to 7 days, and it was the highest when the scratched cells consumed the media treated-7dys (Figure 4). HA-SA-Np significantly (p 0.001-p 0.0001) increased cell migration after 24 hours of scratching (Figure 4). The treated-5dys and treated-7dys media, treated with HA-SA-Np for 5 and 7 days, respectively, had a considerably (p 0.0001) greater migration rate with 100 percent closure than the untreated media. As a result, this finding revealed that releasing silicic acid (silica) from HA-SA-Np was critical in stimulating the healing and migration of human dermal fibroblast cells.

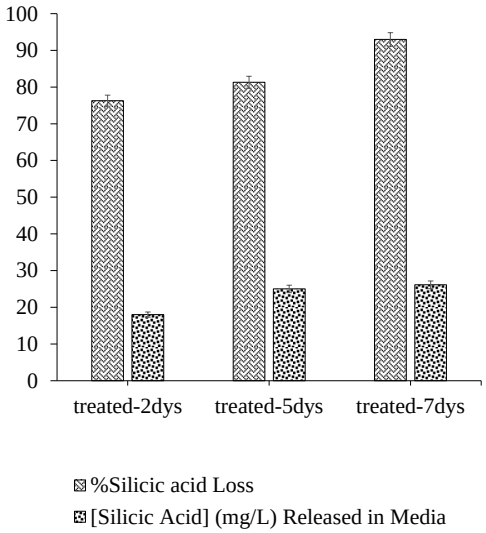

Figure 5. The percentage of silicic acid lost in the media and the amount (mg/L) of silicic acid released into the culturing media following 24 hours of treatment with media-treated HA-SA-Np, at different treating days (2, 5, and 7 days).

Figure 5 depicts how HA-SA-Np's physicochemical properties and resorbability impact the HSF 1184. It was done by determining the amounts of silicic acid (mg/L) released into the media while HSF 1184 cells were present, as well as the percentage of silicic acid lost after 24 hours of incubation. Figure 5 shows the amount of silicic acid released into the medium (mg/L) and its percentage loss following 24 hours of exposure to HA-SA-Np on various treatment days (2, 5, and 7 days).

Figure 5 depicts the release of silicic acid from the HA-SA-Np, with the concentration increasing as the number of days of extraction rose. After a 24-hour incubation period, the percentage of silicic acid lost increased with increasing HA-SA-Np treatment days. Compared to treated-2dys and treated-5dys, almost 95 percent of silicic acid was lost in the media after treatment with treated-7dys. It could be attributable to the silica uptake by the cells [23,24].

On various days, cell proliferation and migration were significantly higher in HA-SA-Nps-treated fibroblast cells than in untreated cells (Figures 3 and 4). These findings confirmed the effect of silicic acid on the observed percentage of cell closure. Furthermore, the results demonstrate that the silicic acid (silica) produced by HA-SA-Np plays an essential role in initiating and enhancing human dermal fibroblast cell repair and migration (Figure 5). The increased proliferation and migration of fibroblast cells suggest that silicic acid's ionic dissolution products boost fibroblast cells' biological response and growth [25].

4. Conclusions

The hydroxyapatite-incorporated silica aerogel nanoparticles (HA-SA-Np) stimulate cell growth, facilitate cell adhesion and dissemination, and improve cell healing and migration in this study. A weight ratio of 0.5 HA/SiO_2 appears to be advantageous for cell growth, and the findings further highlight the need to utilize an adequate HA/SiO_2 weight ratio to enhance fibroblastic development. The results show that the HA-SA-Np stimulates fibroblastic growth and enhances the adhesion, proliferation, and migration of normal human fibroblast cells by concurrently resorbing and releasing an acceptable quantity of silica. As a result, HA-SA-Np can be used by a normal human dermal fibroblast cell as a biocompatible and bio-inductive substance (HSF1184). Additionally, the sol-gel ambient pressure dried HA-SA-Np, generated from rice husk ash, can be used as a carrier and cell delivery vehicle to enhance implant and wound care applications.

Funding

Funding for this study came from the Fundamental Research Grant Scheme (FRGS) under grant number 4F514.

Acknowledgments

The Ministry of Higher Education in Malaysia and Universiti Teknologi Malaysia (UTM) are commended for providing financial support for this research project through the Fundamental Research Grant Scheme (FRGS, Vot No: 4F514).

Conflicts of Interest

The authors disclose no conflicts of interest. The funders played no part in the planning of the study, the gathering, analysis, or interpretation of data, the writing of the paper, or the choice to publish the findings.

References

1. Rakita, A.; Nikolić, N.; Mildner, M.; Matiasek, J.; Elbe-Bürger, A. Re-epithelialization and immune cell behaviour in an ex vivo human skin model. *Sci. Rep.* **2020,** *10*, https://doi.org/10.1038/s41598-019-56847-4.
2. Guastaferro, M.; Reverchon, E.; Baldino, L. Polysaccharide-based aerogel production for biomedical applications: A comparative review. *Mater.* **2021**, *14*, 1631, https://doi.org/10.3390/ma14071631.
3. Sani, N.S; Malek, N.A.N.N.; Jemon, K.; Kadir, M.R.A.; Hamdan, H. *In vitro* bioactivity and osteoblast cell viability studies of hydroxyapatite-incorporated silica aerogel. *J. Sol-Gel Sci. Technol.* **2020**, *96*, 166-177, https://doi.org/10.1007/s10971-020-05386-w.
4. Bianchera, A.; Catanzano, O.; Boateng, J.; Elviri, L. The place of biomaterials in wound healing. In *Therapeutic Dressings and Wound Healing Applications*. Ed. Boatneg, J. John Wiley and Sons Ltd., **2020,** 337-366, https://doi.org/10.1002/9781119433316.ch15.
5. Ocando, C.; Dinescu, S.; Samoila, I.; Ghitulica, C.D.; Cucuruz, A.; Costache, M.; Averous, L. Fabrication and properties of alginate-hydroxyapatite biocomposites as efficient biomaterials for bone regeneration. *Eur. Polym. J.* **2021,** *151*, 110444, https://doi.org/10.1016/j.eurpolymj.2021.110444.
6. Dileep Kumar, V. G.; Sridhar, M. S.; Aramwit, P.; Krut'ko, V. K.; Musskaya, O. N.; Glazov, I. E.; Reddy, N. A review on the synthesis and properties of hydroxyapatite for biomedical applications. *J. Biomater. Sci. Polym. Ed.* **2022**, *33*, 229-261, https://doi.org/10.1080/09205063.2021.1980985.
7. Zhao, R.; Yang, R.; Cooper, P. R.; Khurshid, Z.; Shavandi, A.; Ratnayake, J. Bone grafts and substitutes in dentistry: A review of current trends and developments. *Molecules* **2021**, *26*, 3007, https://doi.org/10.3390/molecules26103007.
8. Buck II, D.W.; Alam, M.; Kim, J.Y. Injectable fillers for facial rejuvenation: A review. *J. Plast. Reconstr. Aesthet. Surg.* **2009**, *62*, 11-18, https://doi.org/10.1016/j.bjps.2008.06.036.
9. Sani, N.S.; Malek. N.A.; Jemon, K.; Kadir, M.R; Hamdan, H. Effect of mass concentration on bioactivity and cell viability of calcined silica aerogel synthesized from rice husk ash as silica source. *J. Sol-Gel Sci. Technol.* **2017,** *82*, 120-132, https://doi.org/10.1007/s10971-016-4266-y.
10. Sonatkar, J.; Kandasubramanian, B. Bioactive glass with biocompatible polymers for bone applications. *Eur. Polym. J.* **2021,** *160*, 110801, https://doi.org/10.1016/j.eurpolymj.2021.110801.
11. Yuan, X.; Xu, Y.; Lu, T.; He, F.; Zhang, L.; He, Q.; Ye, J. Enhancing the bioactivity of hydroxyapatite bioceramic via encapsulating with silica-based bioactive glass sol. *J. Mech. Behav. Biomed. Mater.* **2022,** 105104, https://doi.org/10.1016/j.jmbbm.2022.105104.
12. Kim, M.H.; Chalisserry, E.P.; Mondal, S.; Oh, J.; Nam, S.Y. Silicon-substituted hydroxyapatite reinforced 3D printed gelatin membrane for guided bone regeneration. *Mater. Lett.* **2021,** *304*, 130670, https://doi.org/10.1016/j.matlet.2021.130670.
13. Awasthi, S.; Pandey, S.K.; Arunan, E.; Srivastava, C. A review on hydroxyapatite coatings for the biomedical applications: Experimental and theoretical perspectives. *J. Mater. Chem. B.* **2021,** *9*, 228-249, https://doi.org/10.1039/D0TB02407D.
14. Lee, J.H.; Parthiban, P.; Jin, G.Z.; Knowles, J.C.; Kim, H.W. Materials roles for promoting angiogenesis in tissue regeneration. *Prog. Mater. Sci.* **2021,** *117*, 100732, https://doi.org/10.1016/j.pmatsci.2020.100732.
15. Ishikawa, S.; Iijima, K.; Sasaki, K.; Kawabe, M.; Osawa, S.; Otsuka, H. Silica-based nonwoven fiber fabricated by electrospinning to promote fibroblast functions. *Bull. Chem. Soc. Jpn.* **2020,** *93*, 477-481, https://doi.org/10.1246/bcsj.20190318.
16. Chen, Z.J.; Shi, H.H.; Zheng, L.; Zhang, H.; Cha, Y.Y.; Ruan, H.X.; Zhang, Y.; Zhang, X.C. A new cancellous bone material of silk fibroin/cellulose dual network composite aerogel reinforced by nano-hydroxyapatite filler. *Int. J. Biol. Macromol.* **2021,** *182*, 286-297, https://doi.org/10.1016/j.ijbiomac.2021.03.204.
17. Sani, N.S.; Malek, N.A.; Jemon, K.; Kadir, M.R.; Hamdan, H. Preparation and characterization of hydroxyapatite incorporated silica aerogel and its effect on normal human dermal fibroblast cells. *J. Sol-Gel Sci. Technol.* **2019,** *90*, 422-433, https://doi.org/10.1007/s10971-019-04946-z.

18. Sani, N.S.; Malek, N.A.; Jemon, K.; Kadir, M.R.; Hamdan, H. FTIR study on the preliminary development of synthesis methods for hydroxyapatite modified silica aerogel. *Appl. Mech. Mater.* **2015,** *799-800*, 493-499, https://doi.org/10.4028/www.scientific.net/AMM.799-800.493.
19. Zheng, L.; Zhang, S.; Ying, Z.; Liu, J.; Zhou, Y.; Chen, F. Engineering of aerogel-based biomaterials for biomedical applications. *Int. J. Nanomedicine.* **2020,** *15*, 2363, https://doi.org/10.2147/IJN.S238005.
20. Suarez-Arnedo, A.; Torres Figueroa, F.; Clavijo, C.; Arbeláez, P.; Cruz, J. C.; Muñoz-Camargo, C. An image J plugin for the high throughput image analysis of *in vitro* scratch wound healing assays. *PloS One*, **2020,** *15*, e0232565, https://doi.org/10.1371/journal.pone.0232565.
21. Razzaque, M.S. Phosphate toxicity: New insights into an old problem. *Clin. Sci.* **2013,** *120*, 91–97, https://doi.org/10.1042/CS20100377.
22. Ma, S.; Yang, Y.; Carnes, D.L.; Kim, K.; Park, S.; Oh, S.H.; Ong, J.L. Effects of dissolved calcium and phosphorous on osteoblast responses. *J. Oral Implantol.* **2005,** *31*, 61–67, https://doi.org/10.1563/0-742.1.
23. Quignard, S.; Mosser, G.; Boissière, M.; Coradin, T. Long-term fate of silica nanoparticles interacting with human dermal fibroblasts. *Biomater.* **2012,** *33*, 4431–4442, https://doi.org/10.1016/j.biomaterials.2012.03.004.
24. Kalia, P.; Brooks, R.A.; Kinrade, S.D.; Morgan, D.J.; Brown, A.P.; Rushton, N.; Jugdaohsingh, R. Adsorption of amorphous silica nanoparticles onto hydroxyapatite surfaces differentially alters surfaces properties and adhesion of human osteoblast cells. *PLoS One* **2016,** *11*, 1–15, https://doi.org/10.1371/journal.pone.0144780.
25. Shie, M.Y.; Ding, S. J.; Chang, H.C. The role of silicon in osteoblast-like cell proliferation and apoptosis. *Acta Biomater.* **2011,** *7*, 2604–2614, https://doi.org/10.1016/j.actbio.2011.02.023.